DOI: 10.1021/ma100034h

Macromolecules
ARTICLE

Kinetic Study of the Ring-Opening Metathesis Copolymerization of Ionic with Nonionic Cyclooctatetraene Derivatives To Yield Polyacetylene Ionomers

Dean H. Johnston,[†] Lei Gao,[‡] and Mark C. Lonergan*[,‡]

[†]*Department of Chemistry and Biochemistry, Otterbein College, Westerville, Ohio 43081, and* [‡]*Department of Chemistry and The Materials Science Institute, University of Oregon, Eugene, Oregon 97403*

Received January 6, 2010; Revised Manuscript Received February 4, 2010

ABSTRACT: The ion density in ionically functionalized polyacetylenes can be controlled by the ring-opening metathesis copolymerization of functionalized cyclooctatetraene (RCOT) monomers. Studies are reported on the kinetics for copolymerization of anionic (M_A, R = $-CH_2CH_2SO_3^-NMe_4^+$) and cationic (M_C, R = $-CH_2CH_2$-$NMe_3^+CF_3SO_3^-$) RCOTs with a nonionizable RCOT (M_T, R = $-SiMe_3$) initiated by the well-defined tungsten imidoalkylidene catalyst W[CH(*o*-C_6H_4OMe)](NC_6H_5)[$OCCH_3(CF_3)_2$]$_2$(THF). Twenty separate copolymerizations were studied as a function of the mole fraction of ionic monomer in the feedstock. The monomer consumption was observed to follow zero-order behavior over a range of monomer concentration in the M_A-M_T system, whereas it was observed to follow first-order behavior in the M_C-M_T system. The zero-order behavior in the M_A-M_T system was observed to lead to much less drift in polymer composition than predicted by classic copolymerization theory. The initial rates of monomer conversion were determined and used to calculate the copolymer composition curve. The curves exhibited sigmoidal shapes as described by reactivity ratios $r_c = 8 \pm 3$ and $r_T = 4 \pm 2$ for the M_C-M_T system and $r_A = 2.0 \pm 0.3$ and $r_T = 2.3 \pm 0.3$ for the M_A-M_T system. In all cases, the rate of initiation was observed to be slow relative to propagation, and the initiation rate for M_T was observed to be approximately a factor of 4 greater than for the ionic monomers under similar conditions of monomer and catalyst concentration. The observed trends are explained in terms of ion−ion interactions. These interactions are argued to create different local activities of the ionic monomers in the vicinity of an active catalyst center with ultimate ionic monomer as compared to near either the uninitiated catalyst or an active catalyst center with ultimate nonionic monomer. The largest effects are observed in the M_C-M_T system where, in addition to the largest reactivity ratios, the ratio of the overall polymerization rate to the initiation rate increases by a factor of 20 in progressing from the homopolymerization of M_T to that of M_C.

Introduction

A wide range of polyacetylene derivatives have been synthesized using the ring-opening metathesis polymerization (ROMP) of functionalized cyclooctatetraene (RCOT) monomers.[1−3] Polyacetylene ionomers fabricated from the ROMP of ionically functionalized RCOTs[4] have been useful materials in exploring the fundamental electrical and electrochemical properties of ionically functionalized conjugated polymers.[5−8] Copolymerization is an important tool for controlling the ion density in these materials.[9] In this work, we characterize the basic kinetic features in the ring-opening metathesis copolymerization of ionic with nonionic RCOTs initiated by the well-defined Schrock initiator W[CH(*o*-C_6H_4OMe)](NC_6H_5)[$OCCH_3(CF_3)_2$]$_2$(THF) (**1**, with THF = tetrahydrofuran), as shown in Scheme 1. A primary goal is to better understand the compositional uniformity, monomer distribution, and level of structural control obtainable in the direct synthesis of polyacetylene ionomers from RCOT monomers using **1**.

The ring-opening metathesis of ionically functionalized RCOTs spans two areas where ROMP is being explored for the synthesis of high-performance materials, namely, in the fabrication of conjugated polymers and polyelectrolytes. In the area of conjugated polymers, ROMP has been used to fabricate a range of materials by both direct and indirect routes.[10,11] The indirect Durham precursor route to polyacetylene[12,13] is an important early example that paved the way for many studies on polyacetylene and its device physics. Direct routes to polyacetylene and its derivatives began with the ROMP of cyclooctatetraene using a classical metathesis catalyst.[1] This was followed by extensive work on the use of well-defined Schrock catalysts based on early transition metals to initiate the ROMP of RCOTs leading to a wide range of functionalized polyacetylenes.[2,3,14] More recently, it has been demonstrated that certain Grubbs ruthenium-based catalysts can also initiate the ROMP of RCOTs.[15] Beyond polyacetylene, ROMP has been used in the synthesis of a variety of other conjugated polymers by both direct and indirect routes including poly(1,4-phenylenevinylenes),[16−18] poly(cyclopentadienylenevinylene),[19] and poly(1,4-naphthalenevinylenes).[20,21] In regards to the synthesis of polyelectrolytes, both direct and indirect ROMP routes have been used. Examples of precursor routes include the use of protecting group chemistry in the synthesis of carboxylate-functionalized polyelectrolytes[22] and alkylammonium-derivatized poly(norbornene) derivatives[23] and the use of postpolymerization conversion in the synthesis of a conjugated dicarboxylate poly(1,4-phenylenevinylene).[24] Direct routes have been used to fabricate polyelectrolytes using cationic norbornene derivatives[25−29] and in the related polymerization of zwitterionic norbornene-based betaine substrates.[30]

The combination of ionic functionality and conjugation leads to a class of materials known as conjugated ionomers or conjugated polyelectrolytes.[31] Ionic functionality was originally studied as a means of imparting solubility to conjugated polymers.[32−35] More recently, ionic functionality has been of interest

*To whom correspondence should be addressed. E-mail: lonergan@uoregon.edu.

 Published on Web 02/23/2010

Scheme 1. Ring-Opening Metathesis Copolymerization To Yield Polyacetylene Ionomers

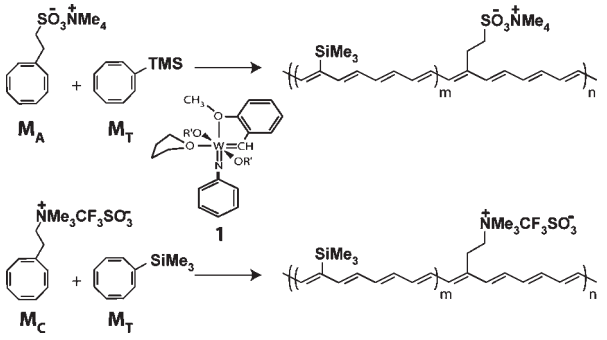

in electronic devices that rely on mixed ionic/electronic conductors. The conjugated backbone in conjugated ionomers provides a pathway for the transport of electronic charge carriers, and the ionizable groups provide the ions necessary to support ionic conductivity. Mixed ionic/electronic conduction in conjugated polymers, both in single-component conjugated ionomers and multicomponent systems, has been of interest in areas such as light emission,[36−40] solar energy conversion,[41,42] and sensing.[43] Conjugated ionomers are also being used to control the doping chemistry of conjugated polymers. The ionizable groups in these materials provide a built-in means of counterbalancing electronic charges injected into the polymer backbone.[44,45] These built-in and covalently bound ions have been used in a self-limiting fashion to control the doping level of conjugated polymers[5,9] and to stabilize interfaces between dissimilarly doped conjugated polymers such as the pn junction.[7] In all of these applications, the control of ion type and density is crucial.

Using the ROMP of ionic RCOTs, it is possible to directly synthesize both anionic and cationic polyacetylene ionomers as shown in Scheme 1.[4] The resulting materials are highly conjugated and solution processable because of the solubilizing influence of the ionic functional groups. This coupled with the fact that oxidatively and reductively doped states are accessible at moderate reduction potentials[5] has made them excellent materials for the fundamental study of conjugated ionomers. Although it has been demonstrated that polyacetylene-based copolymers with varying ion densities can be synthesized using ring-opening metathesis copolymerization,[9] the polymerization kinetics have not been previously studied. Such studies are needed to understand monomer distribution and identify appropriate reaction conditions for the fabrication of polymers with acceptable levels of compositional uniformity. In the homopolymerization of ionically functionalized RCOTs, the presence of ionizable groups strongly influences the polymerization mechanics,[46] and they are expected to have a similarly strong influence on copolymerization.

Experimental Section

Tetramethylammonium 2-cyclooctatetraenylethanesulfonate (M_A) and (2-cyclooctatetraenylethyl)trimethylammonium triflate (M_C) were synthesized as described previously[4] and dried under vacuum for 7 days. Cyclooctatetraenyltrimethylsilane (M_T) was synthesized according to the literature[47] and distilled from calcium hydride. The tungsten catalyst **1** was prepared as described in the literature.[48] Deuteriochloroform was distilled from calcium hydride and freeze−pump−thaw degassed. Hexamethylbenzene (99%, Aldrich) was used as received.

Polymerizations were conducted by mixing deuterated chloroform solutions of the monomers, catalyst, and hexamethylbenzene within a 5 mm diameter NMR tube. The hexamethylbenzene served as an internal standard for quantitative NMR. The tube was introduced into the dark probe of either a Varian INOVA 300 or 500 MHz spectrometer, and time-resolved ^{1}H NMR spectra were recorded at a temperature of 26 ± 1 °C. The spin−lattice relaxation time T_1 for the monomer protons was determined to be ~4 s in O_2-free $CDCl_3$. Correspondingly, spectra were collected with 30 s delay times between acquisitions, and each time point was typically the average of eight acquisitions.

Results

To better understand the results of this study, it is helpful to first describe some results from a previous report on the characterization and electrochemical properties of copolymers isolated from batch polymerizations quenched at early reaction times.[9] From these earlier batch studies, it is known that the ring-opening reaction proceeds with the originally clear, slightly yellow/orange solution turning into an intensely colored, blue/purple heterogeneous mixture with precipitated polymer.The polymer is originally formed in the *cis* form followed by isomerization to the *trans* form, and it remains highly swollen during the polymerization. The isolated polymers were estimated to have M_w in the range of 10−20 kDa by light scattering analysis. Coupled light scattering and size exclusion chromatography was possible only in the M_A−M_T system and yielded polydispersity indexes in the range 1.3−1.9.

The kinetics for the copolymerization of the ionic monomers M_X (M_A or M_C) with M_T were monitored by ^{1}H NMR over a range of compositions.Table 1 shows the reaction conditions studied. As is conventional, square brackets are used to indicate concentrations with the addition of a subscript "0" specifying initial quantities. The mole fraction of ionic monomer in the reaction solution f_X, the instantaneous polymer composition expressed in terms of the mole fraction of ionic monomer in the polymer F_X, and the overall polymerization rate R_p are also tabulated; these quantities are initial values calculated from the early time data of the polymerizations unless explicitly indicated to be a function of time t (e.g., f_X vs $f_X(t)$). Hence, $f_X = [M_X]_0/[M_{tot}]_0$ where $[M_{tot}]_0 = [M_X]_0 + [M_T]_0$. The calculation of F_X and R_p is discussed further below. As in f_X, the subscript "X" is used throughout to indicate quantities associated with either of the ionic monomers; the subscripts "A", "C", and "T" are used to indicate quantities associated with M_A, M_C, and M_T, respectively.

The overall reaction rate was determined by monitoring the disappearance of the seven ring protons on the RCOT monomers in the range 5.7−6.1 ppm. Isolated copolymers redissolved in DMSO or DMF were observed to exhibit a very broad resonance in the range of 5.9−7.3 ppm assigned to the polyacetylene backbone protons. Despite the potential for overlap between the RCOT ring and polyacetylene backbone protons, clean integration of the ring region was possible. The contribution from the already broad polyacetylene backbone protons was further minimized by precipitation of the polymer. Overlap from the polyacetylene backbone protons was only problematic for the most M_T-rich polymerizations during the final 10−15% of the reaction. The results in this work focus primarily on the monomer consumption rates during the initial 10−20% of the reaction. In this region, the contribution from polyacetylene backbone protons was estimated to be less than 5%.

The overall reaction kinetics were noticeably different for the anionic versus the cationic copolymerizations. Figure 1 compares M_A−M_T and M_C−M_T copolymerizations both with $f_X = 0.5$. The data are presented in both zero-order (left ordinate, open circles) and first-order representations (right ordinate, solid circles) with $[M_{tot}]$ normalized by $[M_{tot}]_0$ in both cases. The M_C−M_T copolymerizations were observed to more closely follow a first-order decay with a linear dependence of $\log([M_{tot}]/[M_{tot}]_0)$ on time. In contrast, the M_A−M_T copolymerizations were observed to more closely follow a zero-order decay with a linear

Table 1. Reaction Conditions and Key Results for the Copolymerization of M_T with M_A or M_C[a]

ID	M_X	$[\mathbf{1}]_0$/mM	$[M_X]_0$/mM	$[M_T]_0$/mM	$[M_{tot}]_0$/mM	f_X	F_X	$R_p[\mathbf{1}]_0^{-1}/s^{-1}$
A9	M_A	10	180	0	180	1.00	1.00	2.0×10^{-4}
A8	M_A	16	71	29	99	0.71	0.72	2.4×10^{-4}
A7	M_A	12	61	25	86	0.71	0.76	2.9×10^{-4}
A6	M_A	8.7	67	66	133	0.50	0.51	4.8×10^{-4}
A5	M_A	17	63	109	172	0.37	0.31	5.0×10^{-4}
A4	M_A	29	33	75	109	0.31	0.21	4.5×10^{-4}
A3	M_A	13	14	73	88	0.16	0.10	6.2×10^{-4}
A2	M_A	7.0	61	304	365	0.17	0.09	6.7×10^{-4}
A1	M_A	11	14	135	149	0.10	0.06	6.2×10^{-4}
T0	none	20	0	132	132	0.00	0.00	5.5×10^{-4}
C1	M_C	6.9	28	217	245	0.12	0.07	1.3×10^{-3}
C2	M_C	6.6	47	191	238	0.20	0.11	1.4×10^{-3}
C3	M_C	6.9	81	191	272	0.30	0.23	2.3×10^{-3}
C4	M_C	6.0	97	140	237	0.41	0.55	3.1×10^{-3}
C5	M_C	6.0	243	238	481	0.50	0.55	7.0×10^{-3}
C6	M_C	13	120	120	240	0.50	0.60	2.8×10^{-3}
C7	M_C	7.5	128	120	249	0.52	0.62	3.2×10^{-3}
C8	M_C	7.7	160	85	245	0.65	0.86	5.2×10^{-3}
C9	M_C	8.2	192	51	243	0.79	0.90	5.4×10^{-3}
C10	M_C	6.0	193	35	228	0.85	0.92	5.8×10^{-3}
C11	M_C	7.0	244	0	244	1.00	1.00	6.0×10^{-3}

[a] $[\mathbf{1}]_0$, $[M_X]_0$, $[M_T]_0$, and $[M_{tot}]_0$ are the initial concentrations of catalyst, ionic monomer, M_T, and total monomer, respectively. The f_X is the initial mole fraction of ionic monomer in the feedstock, and F_X is the mole fraction of ionic monomer in the initially formed copolymer. The R_p is the polymerization rate based on total monomer.

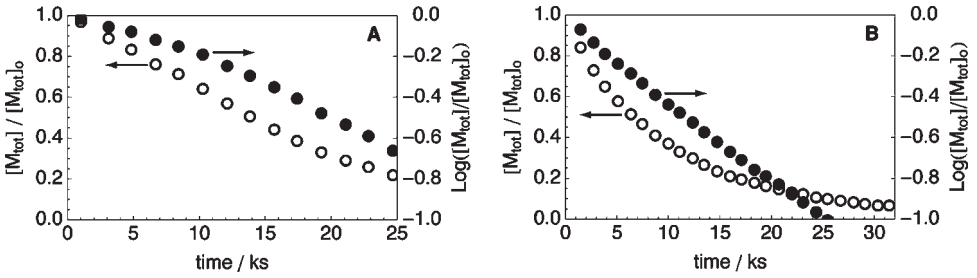

Figure 1. Total monomer concentration $[M_{tot}]$ normalized by the initial monomer concentration $[M_{tot}]_0$ as a function of time for the copolymerization of (A) M_A with M_T at $f_X = 0.50$ (A6 in Table 1) and (B) M_C with M_T at $f_X = 0.52$ (C7 in Table 1). In both cases, the data are presented in both a zero-order representation of $[M_{tot}]/[M_{tot}]_0$ vs time (open circles, left ordinate) and a first-order representation of $\log([M_{tot}]/M_{tot}]_0)$ vs time (closed circles, right ordinate).

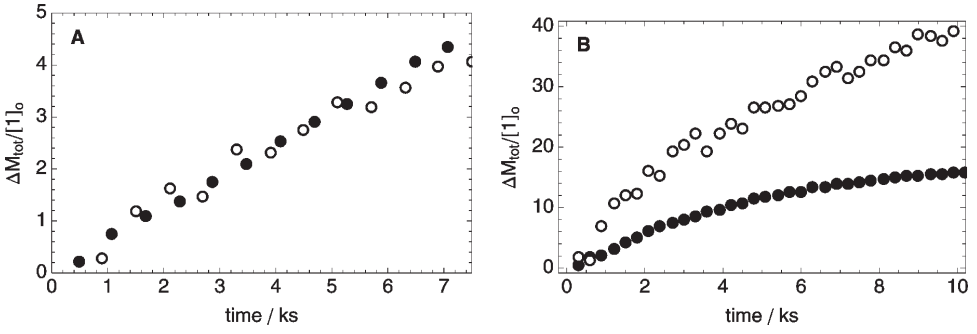

Figure 2. Monomer consumption ($\Delta[M_{tot}] = [M_{tot}]_0 - [M_{tot}]$) normalized by the initial catalyst concentration $[\mathbf{1}]_0$ as a function of time for (A) two copolymerizations of M_A with M_T at $f_x \approx 16$ and $[M_{tot}]_0 = 365$ mM (solid circles, A2 in Table 1) or $[M_{tot}]_0 = 88$ mM (open circles, A3 in Table 1) and (B) two copolymerizations of M_C with M_T at $f_x \approx 0.50$ and $[M_{tot}]_0 = 481$ mM (open circles, C5 in Table 1) or $[M_{tot}]_0 = 249$ mM (closed circles, C7 in Table 1).

dependence of $[M_{tot}]/[M_{tot}]_0$ on time for approximately the first 60% of the reaction. The behavior observed at $f_X = 0.5$ is representative for nearly all of the copolymerizations studied. At the highest values of f_X for the M_C-M_T system, first-order decays were still observed at low conversion, but at high conversion, the initial first-order decay gave way to a second more slowly decaying component.

The decays shown in Figure 1 result from the composite action of initiation, propagation, and termination reactions, and they convolute time and concentration. Consequently, limited studies were performed to expressly address the influence of total monomer concentration on the initial ($t \rightarrow 0$) reaction kinetics. A comparison between systems of differing $[M_{tot}]_0$ at nearly identical f_X was made for low f_X in the M_A-M_T system and for intermediate f_X in the M_C-M_T system. The results from these studies are shown in Figure 2. Quadrupling $[M_{tot}]$ at $f_x \approx 0.16$ for the M_A-M_T system (A2 and A3 in Table 1) resulted in almost no change in the time dependence of the monomer consumption $\Delta[M_{tot}] = [M_{tot}]_0 - [M_{tot}]$, normalized by $[\mathbf{1}]_0$. In contrast, doubling $[M_{tot}]_0$ at $f_x \approx 0.50$ for the M_C-M_T system (C5 and

C7 in Table 1) resulted in $\Delta[M_{tot}]/[\mathbf{1}]_0$ increasing much more rapidly with time. These initial observations led to the M_A-M_T copolymerizations being conducted without specific regard to total monomer concentration, thereby allowing for other dependencies to be explored. They also led to the M_C-M_T system being conducted at near constant total monomer concentration to eliminate $[M_{tot}]_0$ as a variable and isolate the role of f_X. The secondary influence of total monomer concentration on the M_A-M_T copolymerizations is also evident from the near zero-order behavior observed over the first 60% of the reaction. Furthermore, comparison of polymerization A4 and A5 (see Table 1) reveals only a 10% change in overall polymerization rate in response to a nearly 60% change in total monomer concentration at similar values of f_X (0.31 and 0.37).

Linear fits to the early time data for all of the copolymerizations were used to calculate an initial rate of monomer consumption or polymerization rate: $R_p = -d[M_{tot}]/dt$ for $t \rightarrow 0$. Such fits were particularly straightforward for the M_A-M_T system because of the observed linear dependence of $[M_{tot}]$ on time to over 50% conversion. The greater curvature in the time-dependent decay of $[M_{tot}]/[M_{tot}]_0$ for the M_C-M_T system required that the data be collected with greater time resolution and for R_p to be calculated only over the earliest time points where $[M_{tot}]/[M_{tot}]_0$ vs t could be approximated as linear. The $R_p/[\mathbf{1}]_0$ was found to depend on f_X for both the M_A-M_T and M_C-M_T copolymerizations as shown in Figure 3. In the case of M_A-M_T (closed circles), a relatively smooth transition was observed between the higher $R_p/[\mathbf{1}]_0$ for the homopolymerization of M_T to the lower value for M_A as f_X increased. In the case of M_C-M_T (open circles), the transition went in the opposite direction with $R_p/[\mathbf{1}]_0$ increasing with f_X to the faster homopolymerization rate of M_C. It is noted

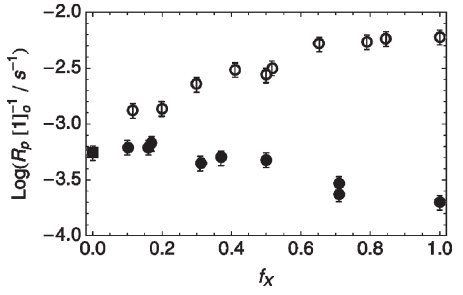

Figure 3. Polymerization rate R_p normalized by the initial catalyst concentration $[\mathbf{1}]_0$ as a function of the mole fraction of ionic monomer in the feedstock f_X for the copolymerization of M_A with M_T (solid circles) and M_C with M_T (open circles). For the M_C-M_T system, the one polymerization conducted at substantially different $[M_{tot}]_0$ is not shown (C5 in Table 1). The polymerization rate for the homopolymerization of M_T is shown as the solid square. The complete reaction conditions for all of the polymerizations are shown in Table 1.

that the slower polymerization rate for the M_A-M_T system and the zero-order dependence on monomer concentration for certain conditions (e.g., Figure 2) necessitated the use of relatively small monomer to catalyst ratios so that a significant percent change in monomer concentration could be observed within a reasonable time frame.

The relative rates of polymerization for the two monomers in a copolymerization dictate the resulting copolymer composition. Hence, the initial reaction rate of the ionic monomer M_X and M_T in each of the polymerizations was quantified as a function of f_X. For both M_A and M_C, the consumption of the ionic monomers was measured by following the disappearance of the resonance due to the methylene protons near 3.0 ppm, which shifted to 3.2 ppm upon ring-opening. The ring protons for the RCOT monomers studied fall into two regions: i: 5.67−5.90 ppm and ii: 5.90−6.04 ppm, with the following distributions: M_T(i:4 ^{1}H, ii:3 ^{1}H); M_A(i:7 ^{1}H, ii:0 ^{1}H); M_C(i:6 ^{1}H, ii:1 ^{1}H). Hence, the $[M_T]$ could be cleanly quantified by integration of region ii for the M_A-M_T system. For the M_C-M_T system, the $[M_T]$ was quantified by integration of region ii followed by subtraction of the M_C component derived from integration of the methylene resonance used to quantify $[M_C]$. This latter approach was, to within experimental error, equivalent to determining $[M_C]$ and $[M_T]$ from the ring protons alone by analyzing the integral ratio between regions i and ii.

Representative decays for M_X and M_T are shown at two different values of f_X for the M_A-M_T system in Figure 4 and for the M_C-M_T system in Figure 5. The maximum time shown in each plot corresponds to ~80% total monomer conversion. As with the time dependence of $[M_{tot}]$, the $[M]/[M]_0$ for each of the monomers was observed to decay linearly in t to at least 50% conversion for the M_A-M_T system. Greater curvature was generally observed for both monomers in the M_C-M_T system except for larger values of f_X as in Figure 5A. For these larger f_X copolymerizations, M_C was still observed to follow a first-order decay, but the minor M_T component exhibited more linear zero-order decays.

The relative rates of monomer consumption in each of the two systems were used to estimate the initial polymer composition formed as a function of f_X. Specifically, the mole fraction of ionic monomer in the initially formed copolymer F_X was determined from the relative rates of monomer consumption: $F_X = R_X/(R_X + R_T)$, where $R_X = -d[M_X]/dt$ and $R_T = -d[M_T]/dt$ both taken in the limit of $t \rightarrow 0$. The solid lines in Figures 4 and 5 show fits to the early time data from which F_X was calculated. The dependence of F_X on f_X was observed to be nonlinear as shown in Figure 6. For both the M_A and M_C systems, the ionic composition of the polymer was found to be enriched relative to the monomer feedstock composition ($F_X > f_X$) for large f_X and diminished ($F_X < f_X$) for small f_X.

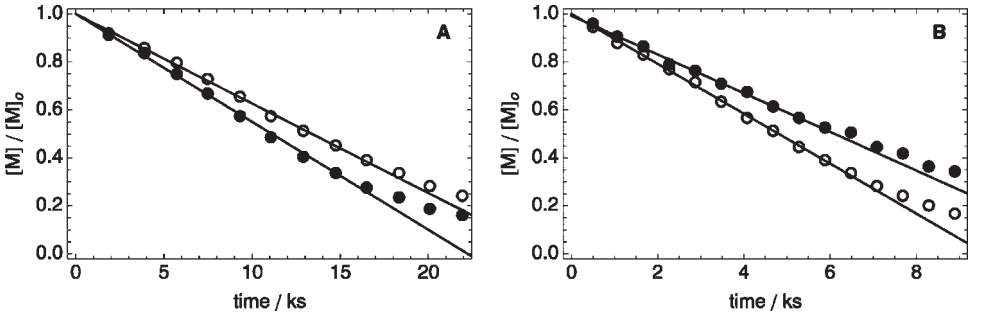

Figure 4. Time dependence of the individual monomer concentrations [M] normalized by their initial concentrations $[M]_0$ for the copolymerization of M_A with M_T at two different values of f_X: (A) $f_X = 0.71$ (A7 in Table 1) and (B) $f_X = 0.16$ (A3 in Table 1). The concentration of the ionic monomers are shown as solid circles in each plot and the concentration of M_T as open circles. The maximum time shown in each plot corresponds to ~80% total monomer conversion. The solid lines show the fits to the experimental data that were used to determine the initial rate of monomer consumption.

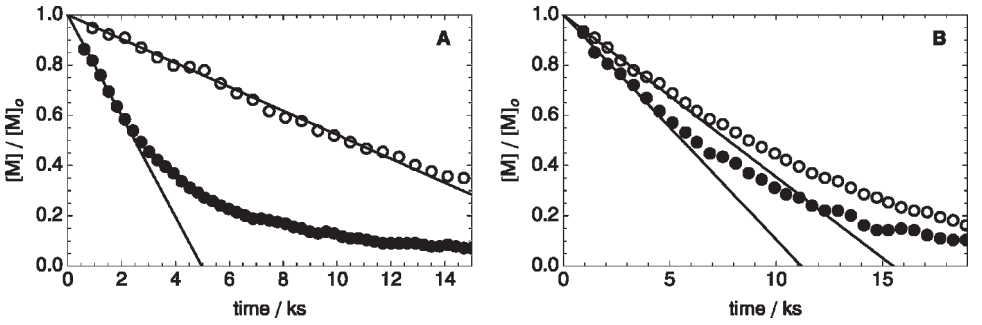

Figure 5. Time dependence of the individual monomer concentrations [M] normalized by their initial concentrations $[M]_0$ for the copolymerization of M_C with M_T at two different values of f_X: (A) $f_X = 0.65$ (C8 in Table 1) and (B) $f_X = 0.30$ (C3 in Table 1). The concentration of the ionic monomers are shown as solid circles in each plot and the concentration of M_T as open circles. The maximum time shown in each plot corresponds to ~80% total monomer conversion. The solid lines show the fits to the experimental data that were used to determine the initial rate of monomer consumption.

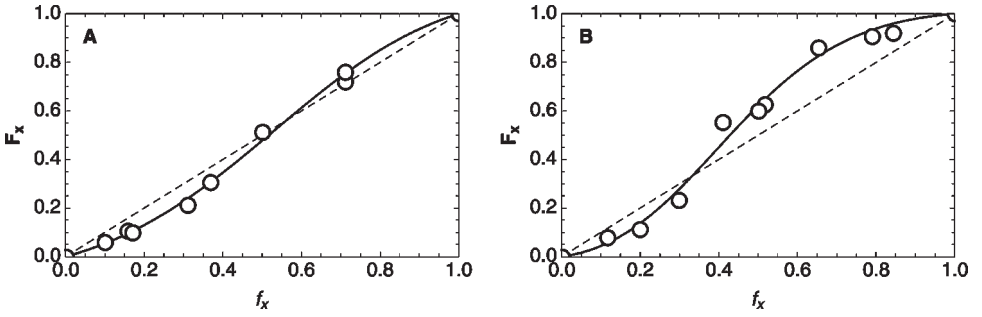

Figure 6. Copolymer composition curves showing the mole fraction of ionic monomer in the initially formed polymer F_X as a function of that in the monomer feedstock f_X for the copolymerization of M_A with M_T in (A) and M_C with M_T in (B). The solid lines are best fits to the copolymer eq 1, and the dashed lines are $F_X = f_X$. The estimated error in F_X is represented by the size of the points.

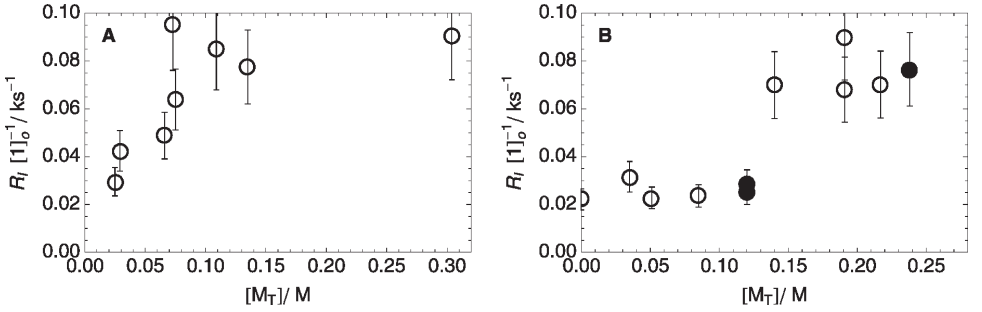

Figure 7. Rate of catalyst initiation R_i normalized by the initial catalyst concentration $[\mathbf{1}]_0$ for (A) the copolymerization of M_A with M_T and (B) the copolymerization of M_C with M_T. In (B), the solid symbols are to highlight the three measurements with $f_X \approx 0.5$.

The copolymer composition curves of Figure 6 were fit to the classic copolymer equation to determine reactivity ratios:[49−51]

$$F_X = \frac{r_X f_X^2 + f_X f_T}{r_X f_X^2 + 2 f_X f_T + r_T f_T^2} \quad (1)$$

where r is the reactivity ratio. The fits were accomplished using a nonlinear least-squares method, and they are shown as the solid lines in Figure 6. The reactivity ratios determined from the fits are $r_A = 2.0 \pm 0.3$, $r_T = 2.3 \pm 0.3$ for $M_A - M_T$ and $r_C = 8 \pm 3$, $r_T = 4 \pm 2$ for $M_C - M_T$.

In addition to the time dependence of the individual monomers in the copolymerizations, it was also possible to follow aspects of catalyst initiation as well. Upon initiation, the singlet benzylic alkylidene resonance is expected to be replaced by a doublet corresponding to the alkylidene resonance of the growing polyacetylene chain. In most experiments, the doublet characteristic of the active propagating alkylidene was not observed. Rather, only the singlet of the uninitiated alkylidene was observed, and its intensity decreased throughout the polymerization. Two experiments were performed in a higher field instrument with the sole purpose of identifying the propagating alkylidene (A3 and A7 in Table 1). In these experiments, a doublet was indeed observed at 11.48 ppm. Its intensity was estimated to be less than 3% of the initial alkylidene resonance of the uninitiated catalyst, and its time-dependent concentration could not be accurately quantified. The concentration of the uninitiated catalyst could however be successfully monitored by quantification of the benzylic alkylidene resonance. The initial rate of catalyst initiation, $R_i = -d[\mathbf{1}]/dt$, was calculated from the slope of linear fits to the early time data.

The R_i was observed to depend on the $[M_T]$ over certain regions as shown in Figure 7. Although the data are noisy due to the relatively small intensity of the alkylidene resonance, it is clear that R_i was the greatest for samples with the highest $[M_T]$. For both copolymerization systems, it also appears that R_i saturates at high $[M_T]$, becoming independent of $[M_T]$. The data of Figure 7 could be alternatively presented in terms of f_X rather than $[M_T]$.

The [M_T] representation was deemed more appropriate primarily because of the comparison between copolymerizations C5 and C7 (see Table 1) which were conducted at constant f_X but differing values of [M_T]. The factor of 2 difference in their R_i (and for that matter their R_p) suggests that [M_T] is the more natural variable.

The ratio R_p/R_i is the kinetic chain length ν. This ratio was in the range of 10−200, calculated from the early time values of R_p and R_i, with the larger values in the M_C-M_T system. The observed range of ν predicts number-average molecular weights in the range M_n = 3−70 kDa. As mentioned earlier, previous studies on batch polymerizations showed that copolymer and homopolymer samples isolated during the first 20% of the reaction had weight-average molecular weights M_w in the range of 10−20 kDa by light scattering. The M_n from ν and M_w from light scattering are qualitatively consistent, especially considering contributions from polydispersity, that the two determinations were conducted at different points in the reaction, and the challenges in the accurate molecular weight characterization of isolated polyacetylene ionomers.

Discussion

The nonunity reactivity ratios characterizing the sigmoidal shape of the composition curve in Figure 6 have two important consequences. The first is the nonrandom incorporation of monomers into the polymer chain. The second is the compositional drift in the reaction solution or polymer that occurs when the instantaneous polymer composition does not match the monomer feedstock composition. First, the statistical distribution of monomers within the polymer is discussed. This discussion assumes the terminal model whereby the probability of incorporating a particular monomer depends only on the last (terminal) monomer added to the growing chain. In this case, the reactivity ratios are related to the conditional probabilities for the sequences M_XM_T and M_TM_X, P_{XT} and P_{TX} by[52,53]

$$P_{XT}^{-1} = 1 + \frac{f_X}{1-f_X} r_X, \quad P_{TX}^{-1} = 1 + \frac{1-f_X}{f_X} r_T \qquad (2)$$

The greater than unity reactivity ratios indicate a preference for the repeated insertion of a given monomer. The reactivity ratios can be used to predict the average number of uninterrupted monomers of type y, $\bar{n}_y$. At the relatively low value of F_X = 0.15, the terminal model predicts $\bar{n}_C$ = 2.4 and $\bar{n}_A$ = 1.3 for the M_C-M_T and M_A-M_T systems, respectively. For comparison, the average block size of ionic monomers in a random distribution at F_X = 0.15 is $\bar{n}_X$ = 1.2.

At low ion densities, it is not only the $\bar{n}_y$ for the minority component that is important. The majority component is also important because of the finite molecular weight of the samples. The molecular weight of copolymer samples isolated near 20% conversion and over a range of F_X was in the range M_w = 10−20 kDa. As $\bar{n}_y$ for the majority component approaches the chain length, the formation of homopolymer chains becomes inevitable. Once this occurs, there is little advantage to the copolymerization of RCOTs relative to the simple fabrication of polymer blends. The terminal model for the situation of F_X = 0.15 discussed above predicts $\bar{n}_T$ = 24 and $\bar{n}_T$ = 14 for the M_C-M_T and M_A-M_T systems, respectively. For comparison, the average block size of M_T monomers in a random distribution at F_X = 0.15 is $\bar{n}_T$ = 6.6. The $\bar{n}_T$ = 24 block corresponds to M_n = 1.8 kDa, and the $\bar{n}_T$ = 14 block corresponds to M_n = 1.1 kDa. Even considering polydispersity, the $\bar{n}_T$ remains small relative to the average chain length at F_X = 0.15. For polymers synthesized with F_X < 0.10, however, the block length of the majority component is expected to approach the chain length, and a significant number of homopolymer chains of M_T are predicted.

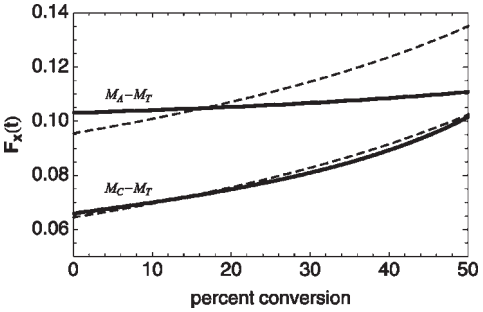

Figure 8. Polymer composition $F_X(t)$ as a function of percent conversion for f_X = 0.16 in the M_A-M_T system (upper pair of curves) and f_X = 0.12 in the M_C-M_T system. The solid lines are calculated from derivatives of polynomial fits to the experimental monomer concentration vs time data. The dashed lines are calculated from the copolymer composition curve determined from the initial rate data (Figure 6) and assuming this composition curve holds for the entire reaction.

The information on monomer distribution derived from the kinetic data is important to studies on the electronic properties of polyacetylene ionomers. A motivation for studying conjugated ionomers in organic electronics is the use of ionic functionality to control the spatial distribution of charge.[6,7] The chain sequence and any resulting microphase separation ultimately determine the spatial distribution of ionic monomers in bulk polymer samples, which in turn helps shape the electric field distribution driving charge transport and injection under bias. The simplest situation would be where the ionic centers act independently, but any ion pairing or clustering may lead to more complicated correlated behavior. The reactivity ratios indicate that, in particular for the M_C-M_T system, ionic monomers have a tendency to group together. Given that the highest reversible dopant density that can be achieved in substituted polyacetylenes is estimated to be one injected charge (electron or hole) per 12−16 double bonds,[3,5] any local pairing of ionic monomers may prevent the preparation of precisely internally compensated doped states where the density of injected charge is precisely balanced by the density of covalently bound ionic centers. Rather, excess mobile ions may be present because their *local* density in the undoped material is greater than the reversible dopant density achievable. Precisely internally compensated states are pure electronic conductors, making them more analogous to doped inorganic semiconductors than conventional doped conjugated polymers, which are mixed ionic/electronic conductors.

The deviation of the copolymerization from the ideal case with $r_X = r_T = 1$ indicates that f_X changes during the course of the polymerization because the composition of the polymer formed during the polymerization does not generally match the feedstock composition. This drift can be calculated from and is clearly evident from the different functional forms of the [M]/[M]$_0$ vs t in Figures 4 and 5. Traditionally, reactivity ratios provide a convenient means of parametrizing the nonrandom incorporation of monomers and hence the resulting drift in both $f_X(t)$ and $F_X(t)$. Because of some unusual aspects (see below) of the ROMP of ionic RCOTs, a comparison was made between the drift in the instantaneous polymer composition determined directly from the rate data at different time points of the reaction and that calculated in the standard way from reactivity ratios determined from the initial rate data.

Figure 8 compares $F_X(t)$ calculated from the time-dependent rate data with that theoretically derived from the composition curves of Figure 6. The comparison was made in a composition range where the largest drift in the content of ionic monomer is expected. There is relatively good agreement in the M_C-M_T system, whereas there is less compositional drift than theoretically predicted in the M_A-M_T system. The reduced compositional drift

in the M_A-M_T system is a consequence of the zero-order kinetics observed for each monomer over a substantial portion of the polymerization. Over the period where the monomers are consumed at a constant rate (zero-order behavior), the instantaneous polymer composition will not shift despite changing reaction conditions.

The above discussion raises an apparent contradiction. The composition curve of Figure 6 for the M_A-M_T system illustrates a dependence of F_X on f_X. The zero-order reaction kinetics indicate that the rate of monomer consumption, and hence $F_X(t)$, does not change despite a changing $f_X(t)$ at least for some portion of the copolymerization. These two observations are reconciled if the composition curve itself changes during the course of the reaction. Such a change could occur if the statistics of monomer incorporation depend not only on the monomer feedstock composition but also on other aspects of the reaction solution. A pristine solution of monomers of given concentrations is not identical to a polymerization solution that achieves the same monomer concentrations during the course of a reaction. Most notable for the polymerization of ionic RCOTs, these two solutions can differ in ionic strength. For instance, a monomer feedstock initially with $f_X = 0.5$ will have a lower total ionic strength than a reaction that begins with a monomer feedstock of $f_X = 0.75$ (same $[M_{tot}]_0$) and later drifts to $f_X(t) = 0.5$, if it is assumed that any formed polymer still contributes to the ionic strength. Polymer chains present in the reaction solution can still contribute to ion-pairing equilibria and hence influence the activity of the monomers. A distinction between the composition curve determined based on initial rate data and that governing the entire time course of the polymerization is reminiscent of observations made in the homopolymerizations of M_A and M_C. The initial rate in these systems shows a zero-order dependence on the initial monomer concentration, whereas the monomer decays show a first-order dependence on monomer concentration.[46]

In previous experiments on the properties of isolated copolymers,[9] polymerizations were intentionally quenched after less than 20% conversion in an effort to balance yield with compositional uniformity. The reactivity ratios and kinetic data now provide for an estimate of the compositional uniformity expected in these polymers. The isolated polymers were synthesized from monomer solutions with $0.1 < f_X < 0.5$ because of interest in low F_X polymers. For the M_C-M_T system, the compositional drift can be calculated from the composition curves in the standard manner. Based on eq 1, the drift in $F_X(t)$ for the M_C-M_T system from 0 to 20% conversion is expected to be 20% for $f_X = 0.1$ and 7% at $f_X = 0.5$. For the M_A-M_T system, the kinetic data indicate that $F_X(t)$ during the first 20% of the copolymerization drifts less than 3% over the range $0.1 < f_X < 0.5$.

Above, the implications of the nonideal composition curve was discussed without specific reference to the nature of the monomers. The fact that M_C and M_A are ionizable creates the possibility for ion-pairing and clustering equilibria. Such equilibria provide a logical explanation for the observed reactivity ratios and other aspects of the polymerization, and they are expected because the copolymerizations were conducted in $CDCl_3$, which has a relatively low dielectric constant.[55,56] Ion clustering away from the uninitiated, nonionic catalyst could limit the activity of the monomers in regards to initiation with the nonionic catalyst, consistent with the observation that the ionic monomers initiate more slowly than M_T. Once initiated, clustering around a terminal ionic monomer may increase the local activity of that monomer at the expense of the local activity of M_T, consistent with $r_X > 1$ in both systems. Invoking a different monomer concentration or activity in the vicinity of the propagating chain relative to that in the bulk solution is similar to the approach taken in describing solvent effects on the radical copolymerization of polar with nonpolar monomers.[57,58] The invocation of ion−ion interactions as an important element in describing chain propagation is also reminiscent of the important role ion−ion interactions play in describing the kinetics of ionic polymerizations.[59,55] Ion pairing has also been proposed to explain various aspects of the homopolymerizations of M_C and M_A. In particular, ion pairing has been invoked to explain why the addition of an inert salt inhibits the polymerization of M_C, whereas it has no effect on the polymerization rate of M_T.[46]

The overall polymerization rate is more complicated because it is the product of the initiation, propagation, and termination steps. The ROMPs herein are not a controlled or "living" system. Rather, initiation, propagation, and termination reactions are not well separated in time. This is most apparent herein from the observation that never more than 50% of the catalyst is initiated, even after the near complete conversion of an excess of monomer. The presence of termination reactions is evident from the observation that the concentration of the propagating alkylidene remains much smaller than the total concentration of catalyst initiated. As the system is not living and it was not possible to reliably quantify the propagating species, it is not possible to independently measure and hence rigorously discuss the propagation and termination reactions. Nevertheless, the substantial change in $R_p/[\mathbf{1}]_0$ with the mole fraction and nature of the ionic monomer (see Figure 3) again illustrates the substantial role ionic functionality has on the ROMP of RCOTs. In particular, the substantial increase in $R_p/[\mathbf{1}]_0$ with increasing f_X in the M_C-M_T copolymerizations despite the decreasing initiation rate is consistent with a large increase in the local activity of ionic monomers available for propagation. Specifically, the ratio R_p/R_i was observed to increase by a factor of 20 in going from the homopolymerization of M_T to that of M_C. In the M_A-M_T system, the R_p roughly tracked with R_i. The fact that the largest effect was observed in the M_C-M_T system is consistent with r_C being the largest of the reactivity ratios observed.

Summary

A study of the kinetics for the ring-opening metathesis copolymerization of ionic with nonionic RCOTs as a function of the mole fraction of ionic monomer was presented. The results suggest that ion−ion interactions play an important role in both the initiation and propagation reactions in a manner that can be summarized as follows. Ion clustering increases the density of ionic monomers near the active catalyst center when the ultimate monomer is charged. This leads to enhanced propagation relative to initiation and reactivity ratios greater than one for the ionic partner of the copolymerization pair. At the same time, ion clustering decreases the density of ionic monomers near the catalyst when the ultimate monomer is uncharged or the catalyst is uninitiated. The observations of reactivity ratios greater than unity imply through the terminal model compositional drift of the monomer feedstock and a nonrandom distribution of monomers within the polymer chain. As in classic copolymerizations, the drift in the monomer feedstock translates into a drift in the polymer composition for the M_C-M_T system, but owing to zero-order kinetics, minimal compositional drift is observed in the M_A-M_T system. The nonrandom distribution of monomers corresponds to a tendency for ionic monomers to group together, which may be an important consideration in efforts to understand and control the doping chemistry of polyacetylene ionomers. The importance of ionic interactions also point to the possibility that additional control over polymer structure can be achieved by controlling the dielectric and ionic environment of the copolymerizations. With such control, it may be possible to develop syntheses with less compositional drift or additional control over monomer distribution. It is not likely, however, that manipulating factors such as solvent dielectric constant or ionic strength will overcome a key limitation in the ROMP of RCOTs

initiated by **1**, namely, slow initiation relative to propagation. It is likely that moving these polymerizations closer to a controlled system will require new catalyst design.

Acknowledgment. This work was support by the NSF Division of Materials Research (DMR-0519489). The authors thank Stephen Robinson and David Stay for helpful comments.

References and Notes

(1) Korshak, Y. V.; Korshak, V. V.; Kanischka, G.; Hoecker, H. *Makromol. Chem., Rapid Commun.* **1985**, *6*, 685.
(2) Klavetter, F. L.; Grubbs, R. H. *J. Am. Chem. Soc.* **1988**, *110*, 7807.
(3) Gorman, C. B.; Ginsburg, E. J.; Grubbs, R. H. *J. Am. Chem. Soc.* **1993**, *115*, 1397.
(4) Langsdorf, B. L.; Zhou, X.; Adler, D. H.; Lonergan, M. C. *Macromolecules* **1999**, *32*, 2796.
(5) Lonergan, M. C.; Cheng, C. H. W.; Langsdorf, B. L.; Zhou, X. *J. Am. Chem. Soc.* **2002**, *124*, 690.
(6) Cheng, C. H. W.; Boettcher, S. W.; Johnston, D. H.; Lonergan, M. C. *J. Am. Chem. Soc.* **2004**, *126*, 8666.
(7) Cheng, C. H. W.; Lonergan, M. C. *J. Am. Chem. Soc.* **2004**, *126*, 10536.
(8) Cheng, C. H. W.; Lin, F. D.; Lonergan, M. C. *J. Phys. Chem. B* **2005**, *109*, 10168.
(9) Gao, L.; Johnston, D.; Lonergan, M. C. *Macromolecules* **2008**, *41*, 4071.
(10) Stelzer, F.; Muelner, R.; Schlick, H.; Leising, G. In *Ring Opening Metathesis Polymerization and Related Chemistry*; Khosravi, E., Szymanska-Buzar, T., Eds.; Kluwer Academic Publishers: Dordrecht, 2000; Vol. *56*, p 185.
(11) Feast, W. J. In *Handbook of Metathesis*; Grubbs, R. H., Ed.; Wiley-VCH: Weinheim, 2003; Vol. *3*, p 118.
(12) Edwards, J. H.; Feast, W. J. *Polymer* **1980**, *21*, 595.
(13) Edwards, J. H.; Feast, W. J.; Bott, D. C. *Polymer* **1984**, *25*, 395.
(14) Moore, J. S.; Gorman, C. B.; Grubbs, R. H. *J. Am. Chem. Soc.* **1991**, *113*, 1704.
(15) Scherman, O. A.; Grubbs, R. H. *Synth. Met.* **2001**, *124*, 431.
(16) Miao, Y. J.; Bazan, G. C. *J. Am. Chem. Soc.* **1994**, *116*, 9379.
(17) Thorn-Csanyi, E.; Hohnk, H. D. *J. Mol. Catal.* **1992**, *76*, 101.
(18) Thorn-Csanyi, E.; Hohnk, H. D.; Pflug, K. P. *J. Mol. Catal.* **1993**, *84*, 253.
(19) Schimetta, M.; Stelzer, F. *Macromolecules* **1994**, *27*, 3769.
(20) Tasch, S.; Graupner, W.; Leising, G.; Pu, L.; Wagner, M. W.; Grubbs, R. H. *Adv. Mater.* **1995**, *7*, 903.
(21) Pu, L.; Wagaman, M. W.; Grubbs, R. H. *Macromolecules* **1996**, *29*, 1138.
(22) Schitter, R. M. E.; Jocham, D.; Stelzer, F.; Moszner, N.; Volkel, Th. *J. Appl. Polym. Sci.* **2000**, *78*, 47.
(23) Ilker, M. F.; Schule, H.; Coughlin, E. B. *Macromolecules* **2004**, *37*, 694.
(24) Wagaman, M. W.; Grubbs, R. H. *Macromolecules* **1997**, *30*, 3978.
(25) Mohr, B.; Lynn, D. M.; Grubbs, R. H. *Organometallics* **1996**, *15*, 4317.
(26) Lynn, D. M.; Mohr, B.; Grubbs, R. H. *J. Am. Chem. Soc.* **1998**, *120*, 1627.
(27) Lynn, D. M.; Mohr, B.; Grubbs, R. H.; Henling, L. M.; Day, M. W. *J. Am. Chem. Soc.* **2000**, *122*, 6601.
(28) Gallivan, J. P.; Jordan, J. P.; Grubbs, R. H. *Tetrahedron Lett.* **2005**, *46*, 2577.
(29) Rankin, D. A.; P′Pool, S. J.; Schanz, H.-J.; Lowe, A. B. *J. Polym. Sci., Part A: Polym. Chem.* **2007**, *45*, 2113.
(30) Rankin, D. A.; Lowe, A. B. *Macromolecules* **2008**, *41*, 614.
(31) Pinto, M. R.; Schanze, K. S. *Synthesis* **2002**, 1293.
(32) Patil, A. O.; Ikenoue, Y.; Wudl, F.; Heeger, A. J. *J. Am. Chem. Soc.* **1987**, *109*, 1858.
(33) Yue, J.; Epstein, A. J. *J. Am. Chem. Soc.* **1990**, *112*, 2800.
(34) Child, A. D.; Reynolds, J. R. *Macromolecules* **1994**, *27*, 1975.
(35) Sundaresan, N. S.; Basak, S.; Pomerantz, M.; Reynolds, J. R. *J. Chem. Soc., Chem. Commun.* **1987**, 621.
(36) Pei, Q.; Yu, G.; Zhang, C.; Yang, Y.; Heeger, A. J. *Science* **1995**, *269*, 1086.
(37) Cimrova, V.; Schmidt, W.; Rulkens, R.; Schulze, M.; Meyer, W.; Neher, D. *Adv. Mater.* **1996**, *8*, 585.
(38) Baur, J. W.; Kim, S.; Balanda, P. B.; Reynolds, J. R.; Rubner, M. F. *Adv. Mater.* **1998**, *10*, 1452.
(39) Sun, Q.; Li, Y.; Pei, Q. *J. Disp. Technol.* **2007**, *3*, 211.
(40) Edman, L.; Pauchard, M.; Liu, B.; Bazan, G.; Moses, D.; Heeger, A. J. *Appl. Phys. Lett.* **2003**, *82*, 3961.
(41) Gao, J.; Yu, G.; Heeger, A. J. *Appl. Phys. Lett.* **1997**, *71*, 1293.
(42) Bernards, D. A.; Flores-Torres, S.; Abruna, H. D.; Malliaras, G. G. *Science* **2006**, *313*, 1416.
(43) Mcquade, D. T.; Pullen, A. E.; Swager, T. M. *Chem. Rev.* **2000**, *100*, 2537.
(44) Ikenoue, Y.; Chiang, J.; Patil, A. O.; Wudl, F.; Heeger, A. J. *J. Am. Chem. Soc.* **1988**, *110*, 2983.
(45) Ikenoue, Y.; Uotani, N.; Patil, A. O.; Wudl, F.; Heeger, A. J. *Synth. Met.* **1989**, *30*, 305.
(46) Langsdorf, B. L.; Zhou, X.; Lonergan, M. C. *Macromolecules* **2001**, *34*, 2450.
(47) Cooke, M.; Russ, C. R.; Stone, F. G. A. *J. Chem. Soc., Dalton Trans.* **1975**, 256.
(48) Johnson, L. K.; Virgil, S. C.; Grubbs, R. H.; Ziller, J. W. *J. Am. Chem. Soc.* **1990**, *112*, 5384.
(49) Alfrey, T.; Goldfinger, G. *J. Chem. Phys.* **1944**, *12*, 205.
(50) Mayo, F. R.; Lewis, F. M. *J. Am. Chem. Soc.* **1944**, *66*, 1594.
(51) Wall, F. T. *J. Am. Chem. Soc.* **1944**, *66*, 2050.
(52) Goldfinger, G.; Kane, T. *J. Polym. Sci.* **1948**, *3*, 462.
(53) Farina, M. *Makromol. Chem.* **1990**, *191*, 2795.
(54) Szwarc, M. *Ions and Ion Pairs in Organic Reactions*; Wiley-Interscience: New York, 1972.
(55) Schmitt, B. J.; Schulz, G. V. *Eur. Polym. J.* **1975**, *11*, 119.
(56) Kabisch, G. *Ber. Bunsen-Ges. Phys. Chem.* **1976**, *80*, 602.
(57) Boudevska, H.; Todorova, O. *Makromol. Chem., Macromol. Chem. Phys.* **1985**, *186*, 1711.
(58) Harwood, H. J. *Makromol. Chem., Macromol. Symp.* **1987**, *10*, 331.
(59) Szwarc, M. In *Ions and Ion Pairs in Ionic Polymerization*; Szwarc, M., Ed.; Wiley-Interscience: New York, 1974; Vol. *2*, p 375.